Delayed myelination in a mouse model of fragile X syndrome

Laura K.K. Pacey[1], Ingrid C.Y. Xuan[1], Sihui Guan[1], Dafna Sussman[4], R. Mark Henkelman[4], Yan Chen[2], Christian Thomsen[5] and David R. Hampson[1,3],*

[1]Department of Pharmaceutical Sciences, Leslie Dan Faculty of Pharmacy, [2]Faculty of Medicine and [3]Department of Pharmacology, Faculty of Medicine, University of Toronto, Toronto, ON, Canada, [4]Mouse Imaging Centre (MICE) and the Hospital for Sick Children, Toronto, Canada and [5]Department of Neuroinflammation, Lundbeck Research USA, NJ, USA

Fragile X Syndrome is the most common inherited cause of autism. Fragile X mental retardation protein (FMRP), which is absent in fragile X, is an mRNA binding protein that regulates the translation of hundreds of different mRNA transcripts. In the adult brain, FMRP is expressed primarily in the neurons; however, it is also expressed in developing glial cells, where its function is not well understood. Here, we show that fragile X (Fmr1) knockout mice display abnormalities in the myelination of cerebellar axons as early as the first postnatal week, corresponding roughly to the equivalent time in human brain development when symptoms of the syndrome first become apparent (1–3 years of age). At postnatal day (PND) 7, diffusion tensor magnetic resonance imaging showed reduced volume of the Fmr1 cerebellum compared with wild-type mice, concomitant with an 80–85% reduction in the expression of myelin basic protein, fewer myelinated axons and reduced thickness of myelin sheaths, as measured by electron microscopy. Both the expression of the proteoglycan NG2 and the number of PDGFRα+/NG2+ oligodendrocyte precursor cells were reduced in the Fmr1 cerebellum at PND 7. Although myelin proteins were still depressed at PND 15, they regained wild-type levels by PND 30. These findings suggest that impaired maturation or function of oligodendrocyte precursor cells induces delayed myelination in the Fmr1 mouse brain. Our results bolster an emerging recognition that white matter abnormalities in early postnatal brain development represent an underlying neurological deficit in Fragile X syndrome.

INTRODUCTION

Fragile X Syndrome (FXS), the most common single gene cause of autism, results from an expansion of a CGG repeat in the 5′ untranslated region of the X-linked Fmr1 gene. The Fmr1 gene codes for Fragile X Mental Retardation Protein (FMRP), an mRNA binding protein that regulates the translation, stability and transport of hundreds of mRNAs in the brain (1). Dysregulated protein synthesis is thought to result in many of the biochemical and anatomical phenotypes associated with FXS (2–4).

Human imaging and neuropathological studies have revealed alterations in the cerebellum of persons with FXS that include a reduction in the size of the vermis (5,6) and a loss of Purkinje neurons (7). Both abnormalities have also consistently been shown in individuals with idiopathic autism (8–10). In an MRI analysis of the Fmr1 mouse (fragile X knockout mouse, an animal model of the disorder) brain conducted at PND 30, the most prominent change observed was a reduced volume and loss of neurons in the deep cerebellar nuclei, which together with the vestibular nuclei are the sole output of the cerebellar cortex (11). Two separate studies have recently linked mutations in the autism-associated genes TSC1 and TSC2 in Purkinje neurons of the mouse cerebellum to several autism-like phenotypes (12,13). Together, these findings suggest a role for the cerebellum in the pathology of autism spectrum disorders and FXS.

FMRP levels are high in the central nervous system where it is widely and prominently expressed in adult neurons. FMRP is also expressed in immature astrocytes (14,15) and oligodendrocytes (16), and glial expression of dFMRP is required for proper neuroblast development in the drosophila model of FXS (17). Although white matter abnormalities are well established in

*To whom correspondence should be addressed at: Department of Pharmaceutical Sciences, University of Toronto, 144 College St, Toronto, ON, Canada M5S 3M2. Tel: +1 4169784494; Fax: +1 4169788511; Email: d.hampson@utoronto.ca

autism spectrum disorders and FXS (6,18–20), the effects of loss of FMRP on cells of the oligodendrocyte lineage and on myelin production have not been well studied.

The objective of this study was to examine oligodendrocyte precursor cells (OPCs), oligodendroglia and myelin in the Fmr1 mouse cerebellum throughout development. We report reduced cerebellar volume accompanied by delayed myelination and reduced OPC number over the first 2 weeks after birth. These early postnatal abnormalities could underlie the delayed maturation of neurons and contribute to neuronal dysfunction in the adult FXS brain.

RESULTS

FMRP expression in the mouse cerebellum

In the mouse forebrain, FMRP expression has been shown to be highest during early postnatal periods and to decrease as the brain matures (21). To characterize the time course of FMRP expression in the mouse cerebellum, we examined FMRP expression in cerebellar homogenates from male wild-type C57BL/6 mice at various time points during the first 2 months of life (Fig. 1A and B). FMRP expression was highest during the first two postnatal weeks and began dropping by PND 21. Expression leveled off at about 4 weeks after birth and remained steady through to adulthood. The level of FMRP in the adult cerebellum was ∼50% of the peak level of expression attained between postnatal weeks 1 and 2. The cellular distribution of FMRP in the cerebellum was examined using immunocytochemistry. In the cerebellar cortex, FMRP was expressed in all major neuronal populations—granule cells, Purkinje cells and in interneurons of the molecular layer at all timepoints examined (Fig. 1C). FMRP was also highly expressed in neurons of the deep cerebellar nuclei (data not shown). No FMRP expression was detected in Fmr1 knockout mice (Fig. 1C).

FMRP staining was predominantly found in neurons; however, in the deep cerebellar white matter of PND 7 wild-type mice, $27 \pm 3.5\%$ of cells expressing the OPC marker NG2 co-labeled with FMRP (Fig. 1D) while $27 \pm 2.3\%$ of PDGFRα expressing cells also expressed FMRP (Fig. 1E), suggesting that as many as one-quarter of OPCs may express FMRP in the wild-type cerebellum. The myelin marker myelin basic protein (MBP) was also examined at PND 7. Although anti-MBP labeled predominantly the myelin-rich processes of oligodendrocytes, some oligodendrocyte cell bodies can be identified using MBP immunostaining. In the deep cerebellar white matter of wild-type PND 7 mice, $28 \pm 1.5\%$ of MBP positive cell bodies co-labeled with FMRP (Fig. 1F), indicating that FMRP expression can also be found in more mature oligodendrocytes in the cerebellum at PND 7. Together, these results confirm the expression of FMRP in cells of the oligodendrocyte lineage in the developing cerebellum.

Diffusion tensor imaging shows reduced volume of the Fmr1 mouse cerebellum

Diffusion tensor imaging tracks the position and direction of water molecules in tissues. It is particularly sensitive to myelin and is often referred to as a white matter imaging technique (22). Image registration revealed that PND 7 Fmr1 mice had a

significantly smaller cerebellar volume of $14.78 \pm 1.64 \text{ mm}^3$ compared with the wild-type cerebellar volume of $18.40 \pm 1.66 \text{ mm}^3$ ($P = 0.0001$; Fig. 2A and B). Further analysis of relative brain volume (computed as a fraction of overall brain volume) indicated that the cerebellum in the Fmr1 mice remained small in relative volume (Fig. 2C; false discovery rate = 1%). No statistically significant differences between wild-type and Fmr1 mice were seen in fractional anisotropy or mean diffusion anywhere in the brains.

MBP and 2,3 cyclic nucleotide phosphodiesterase (CNPase) expression display abnormal developmental profiles in the Fmr1 cerebellum

To assess potential changes in oligodendrocytes and the status of myelin, we used an antibody to MBP, a major protein component of myelin (Fig. 3). Four isoforms of MBP, corresponding to 14, 17, 18.5 and 21.5 kDa, can be identified using western blotting. The 17 and 18.5 kDa isoforms were difficult to distinguish separately and were therefore quantified together. Expression of all MBP isoforms was dramatically lower in the Fmr1 cerebellum at PND 7 compared with wild-type mice (Fig. 3A; 14 kDa: $16.1 \pm 1.8\%$ of wild-type, $P = 0.02$; 17/18.5 kDa: $14.0 \pm 5.1\%$, $P = 0.005$; 21.5 kDa: $21.4 \pm 8.4\%$, $P = 0.03$). Immunocytochemical analysis of the PND 7 cerebellum confirmed the substantial under-expression of MBP (Fig. 3B). At PND 15, a significant decrease was seen in the 14 and 17/18.5 kDa bands (Fig. 3C; 14 kDa: $44.0 \pm 9.7\%$, $P = 0.04$; 17/18.5 kDa: $55.5 \pm 8.1\%$, $P = 0.04$). Expression of the 21.5 kDa band was not different between wild-type and Fmr1 ($91.1 \pm 14.2\%$, $P = 0.69$). At PND 30, there was a non-significant decrease in the expression of all three MBP isoforms (Fig. 3D; 14 kDa $83 \pm 8.7\%$ of wild-type, $P = 0.21$; 17/18.5 kDa: 90.1 ± 7.3, $P = 0.34$; 21.5 kDa: $90.0 \pm 8.7\%$, $P = 0.40$).

In contrast to the immature cerebellum, in the cerebellum of 2–4-month-old Fmr1 young adults, MBP expression was significantly elevated compared with wild-type (Fig. 3E; 14 kDa: $133.9 \pm 8.0\%$ of wild-type, $P = 0.02$; 17/18.5 kDa: $134.5 \pm 9.5\%$, $P = 0.03$; 21.5 kDa: $132.4 \pm 6.7\%$, $P = 0.01$). In older adult mice 7–15 months old, MBP expression was not different from wild-type (14 kDa: $114.8 \pm 9.6\%$, $P = 0.35$; 17/18.5 kDa: $91.0 \pm 5.6\%$, $P = 0.47$; 21.5 kDa: $87.7 \pm 7.6\%$, $P = 0.18$; blots not shown) suggesting that the elevation in early adulthood is transient. These results are indicative of delayed myelination in the Fmr1 cerebellum, followed by transient over-compensation in young adulthood.

To evaluate myelination over development in each genotype, we directly compared the expression of MBP in samples from PND 7, 15, 30, 2–4-month and 7–15-month-old wild-type with Fmr1 mice using quantitative western blotting (Fig. 4). For both genotypes, the expression of the three MBP isoforms was low at PND 7, rose robustly by PND 15 and continued to rise until at least PND 30. In both Fmr1 and wild-type mice expression of the different isoforms peaked at different developmental timepoints; expression of the 21.5 kDa isoform peaked at PND 30 then fell drastically in the adult, whereas the 17/18.5 kDa forms plateaued around PND 30 while the 14 kDa form continued to rise modestly into adulthood. Notably, over the first 30 days of cerebellar development, all three isoforms showed a general rightward shift in relative expression levels
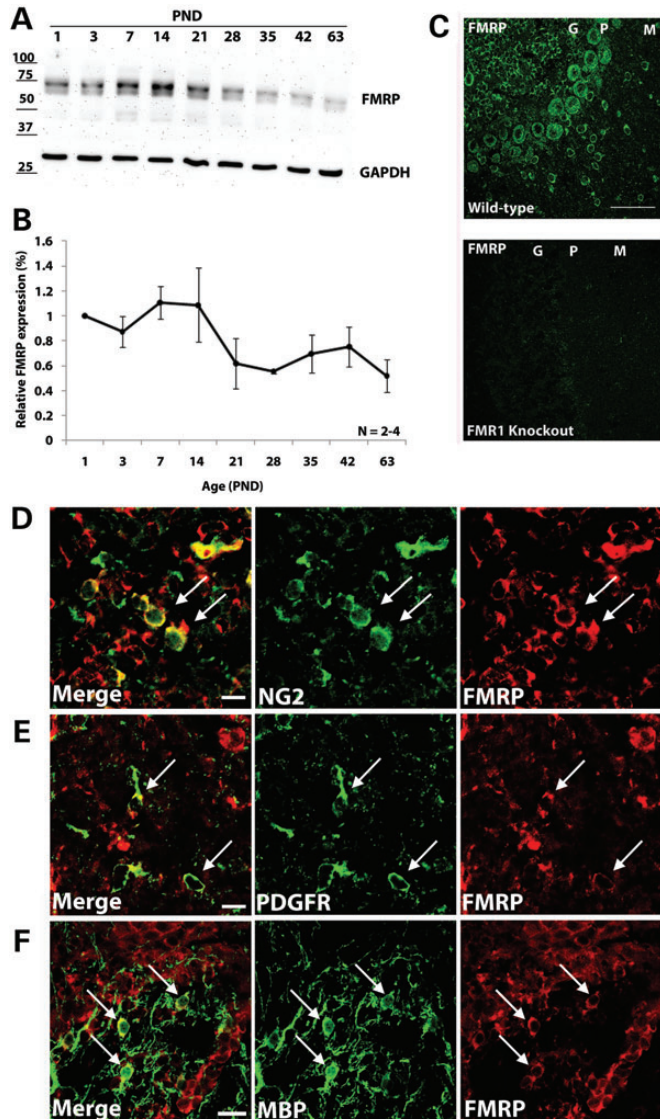
Figure 1. FMRP expression in the developing and mature wild-type mouse cerebellum. (**A**) Representative western blot of cerebellar FMRP expression during postnatal development. (**B**) Mean FMRP expression at each timepoint ($n = 2–4$), expressed relative to PND 1. FMRP expression is highest during the first two postnatal weeks, with expression decreasing to adult levels around PND 28. Error bars represent standard error of the mean. (**C**) Immunofluorescence image of FMRP expression in the cerebellar cortex of the adult wild-type mouse (top); no FMRP expression was detected in the Fmr1 cerebellum (bottom; scale bar = 50 μm). (**D**–**F**) At PND 7, FMRP co-localizes with a population of cells expressing the OPC markers NG2 (D) and PDGFRα (E) in the cerebellar white matter of wild-type mice. FMRP also co-localizes with some cells expressing the oligodendrocyte marker MBP (F) at PND 7. Arrows indicate double-labeled cells. Scale bar = 10 μm for (D) and (E) and 20 μM for (F). G, granular layer; P, Purkinje cell layer; M, molecular layer.

in Fmr1 mice compared with wild-type mice. This finding is consistent with a delay in myelination in the Fmr1 mouse.

Expression of a second myelin marker, CNPase, was also examined in the cerebellum of young wild-type and Fmr1 animals (Fig. 5). At PND 7, CNPase expression was significantly reduced in Fmr1 mice compared with wild-type (Fig. 5A; $24.0 \pm 1.0\%$ of wild-type, $P = 0.04$). At PND 15, there was a

non-significant decrease in CNPase in the Fmr1 cerebellum (Fig. 5B; $86.6 \pm 10.0\%$ of wild-type, $P > 0.05$). CNPase expression was not tested in older animals. These results are consistent with a reduction in myelin in the Fmr1 cerebellum early in development that appears to normalize as the brain matures.

### Reduced myelination in the Fmr1 cerebellum

MBP expression is required for proper myelin formation (23) and loss of MBP results in the absence of compact myelin and the presence of thin myelin sheaths (24). Using electron microscopy, we examined the wild-type and Fmr1 cerebellum at PNDs 7 and 15 to look for structural changes in myelin formation that could result from reduced MBP and CNPase expression (Fig. 6). At PND 7, cerebellar white matter from Fmr1 mice contained significantly fewer myelinated axons compared with matched sections from wild-type mice (Fig. 6C; wild-type: 7.7 ± 0.2 axons/100 μm^2; Fmr1: 5.4 ± 0.8 axons/100 μm^2, $P = 0.04$). The average myelin thickness was also significantly reduced in Fmr1 mice compared with wild-type (Fig. 6D; wild-type: 72.5 ± 2.9 nm, Fmr1: 58.2 ± 4.2 nm, $P = 0.013$). Since the myelin thickness varied widely between individual axons within each mouse, the percentage of axons whose myelin thickness fell within each of five bins was also calculated. This analysis showed a leftward shift in the distribution of myelin thickness in Fmr1 mice, indicating the presence of fewer thick, and more thin sheaths in Fmr1 compared with wild-type mice (Fig. 6E). The G-ratio (diameter of the axon divided by diameter of the axon plus myelin sheath) was also significantly higher in Fmr1 cerebellum compared with wild-type, indicating a thinner myelin sheath in Fmr1 animals (Fig. 6F; wild-type: 0.84 ± 0.007, Fmr1: 0.87 ± 0.001, $P = 0.02$). At PND 7, axon diameter was not different between wild-type and Fmr1 axons (Fig. 6G; WT: 1.23 ± 0.04 μm, Fmr1: 1.20 ± 0.05 μm, $P = 0.43$). At PND 15, there was no significant difference in the number of myelinated axons (Fig. 6J), myelin thickness (Fig. 6K), myelin thickness distribution (Fig. 6L), G-ratio (Fig. 6M) or axon diameter (Fig. 6N) between wild-type and Fmr1 mice. Taken together, these data demonstrate significantly reduced myelination in Fmr1 knockout mice at PND 7.

OPCs are altered in young Fmr1 cerebellum

OPCs are characterized by the expression of NG2 chondroitin sulfate and PDGFRα (25,26). To examine possible causes of delayed myelination in Fmr1 cerebellum, the expression of NG2 was examined via western blots. NG2 expression was significantly reduced in the cerebellum of the Fmr1 mice at PND 7 (Fig. 7A; $68.0 \pm 8.4\%$, $P < 0.05$). In contrast, at PND 15, NG2 expression was elevated in Fmr1 mice (Fig. 7B; $162 \pm 28.4\%$, $P = 0.05$). NG2 expression declines rapidly with development (27) and was not detectable by western blot in the wild-type or Fmr1 cerebellum after PND 15. The observation that NG2 expression is reduced at PND 7 suggests a change in the number or function of OPCs; this result is consistent with the very large reductions in MBP and CNPase at this time point in Fmr1 mice and could account for the delay in myelination.

To further examine the effect of loss of FMRP on OPCs, we labeled cerebellar sections with antibodies to PDGFRα and NG2 and counted the number of cells that expressed both
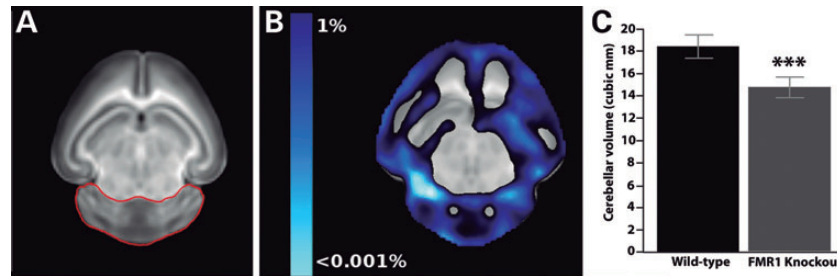
Figure 2. Diffusion tensor imaging of the Fmr1 mouse cerebellum at PND 7. (**A**) A cross-sectional slice showing the cerebral structure visible with DTI. (**B**) The same cross-section overlaid with a color scale-bar highlighting the regions which are statistically smaller in the Fmr1 mouse (in blue) compared with the wild-type controls. Values correspond to the % false discovery rate (FDR). Note that the cerebellum (traced in red in A) is almost completely highlighted (false discovery rate, FDR, value in %). (**C**) Quantification of cerebellar volume (in cubic mm; mean ± SD; $n = 10$ per genotype) demonstrates that the cerebellum of Fmr1 mice is significantly smaller than that of wild-type mice at PND 7. ***$P < 0.001$.

markers at PND 7. At this age, the vast majority of double-labeled cells were restricted to the deep white matter of the cerebellum, with relatively few cells found in the sub-cortical white matter or the cerebellar cortex. In the PND 7 cerebellum, MBP expression in wild-type (and Fmr1) mice was present predominantly in the deep white matter, a finding consistent with previous reports that myelination in the cerebellum is initiated in the deep regions and proceeds outward (28). For these reasons, the number of OPCs was counted only in the deep cerebellar white matter. The number of cells double-labeled with PDGFRα and NG2 was significantly reduced in Fmr1 cerebellum at PND 7 (Fig. 7C; wild-type: 3.9 ± 0.28 cells/1000 μm^2, Fmr1: 2.3 ± 0.5 cells/1000 μm^2, $P = 0.04$). This finding indicates a significant reduction in the number of OPCs in deep white matter of the Fmr1 cerebellum at PND 7. Given that the majority of PDGFRα/NG2 cells and MBP expression were largely restricted to this region at PND 7, it is reasonable to conclude that this reduction in OPC number could account for the reduced myelination observed in Fmr1 mice.

DISCUSSION

The present study demonstrates for the first time an abnormal pattern of myelination in the Fmr1 mouse brain. We found that the normal progression of myelination is delayed in the early postnatal period in the Fmr1 mouse cerebellum, and that the delay may be explained by a reduction in the number of OPCs in the deep cerebellar white matter at this age. The observed abnormalities in the cerebellum become evident by the first postnatal week, a time corresponding to approximately age 1–3 years in humans and the age at which most children with FXS or autism are first diagnosed (29). Neuroimaging studies have consistently demonstrated alterations in white matter volume and structure in the brains of individuals with both FXS and autism (18–20). Hoeft *et al.* (6) reported altered white matter volume in several brain regions of 1–3-year-old boys with FXS; this time frame is analogous to the postnatal period where we observed reduced myelination in the Fmr1 mouse.

### Reduced OPC number can cause delayed myelination

In the CNS, myelin is produced by oligodendrocytes, which extend compacted spirals of membrane around multiple axons. Developmentally, multipotent ventricular stem cells give rise

to committed OPCs, which proliferate to form the pool of cells that eventually become mature oligodendrocytes. We found that the deep cerebellar white matter of Fmr1 mice contained ~40% fewer PDGFRα+/NG2+ cells compared with wild-type mice. Reduced OPC number could contribute to the delayed myelination observed during early postnatal development and could reflect altered OPC survival or a delay in maturation or proliferation.

NG2 is an important regulator of several signaling pathways, including growth factor signaling through PDGFRα (27). The expression of NG2 in the Fmr1 mouse cerebellum was significantly reduced, and similar to the Fmr1 mouse, NG2 knockout mice display delayed myelination which results from delayed OPC proliferation and reduced oligodendrocyte number (26). Although we did not measure proliferation rates in Fmr1 mice, these findings in NG2 knockout mice suggest that diminished OPC proliferation might also be a cause of fewer OPCs in Fmr1 mice. OPC differentiation occurs when the number of OPCs reaches a critical density (30). Therefore, reduced or delayed OPC proliferation could impede OPC differentiation resulting in the delayed myelination observed in Fmr1 mouse cerebellum.

Proper myelination relies on bi-directional signaling between oligodendrocytes and axons (31). Neuronal pathology is well established in FXS but the present study raises the question of whether delayed myelination reflects an axonal or glial deficit. Axon diameter can regulate myelin thickness (32) and whether an axon is myelinated (33). We saw no difference in axon diameter in Fmr1 mice at PND 7 or 15 using electron microscopy. Expression of the axon-specific neurofilament-H was also not different between Fmr1 and wild-type mice at PND 7 (data not shown). These findings suggest the myelination defect is not related to changes in axonal structure. The observation that FMRP is expressed in OPCs and oligodendrocytes in wild-type animals, and the deficiencies in OPC number and NG2 expression discussed earlier also suggest that the pathology in Fmr1 cerebellum is related, at least in part, to changes in the oligodendrocyte lineage cells in the absence of FMRP.

Promising pharmacotherapies for FXS currently being studied in the clinic include Group I metabotropic glutamate receptor (mGluR) antagonists and GABA$_B$ receptor agonists (4,34,35). Interestingly, OPCs have been shown to express both mGluR5 (36) and GABA$_B$ receptors (37) and the GABA$_B$ receptor agonist R-baclofen was shown to increase OPC
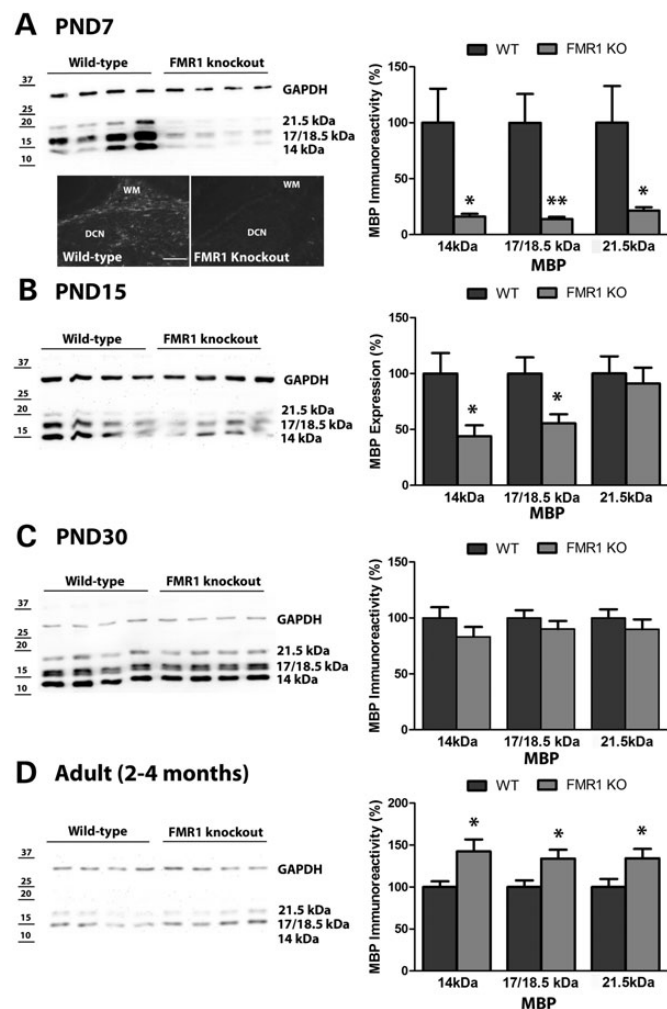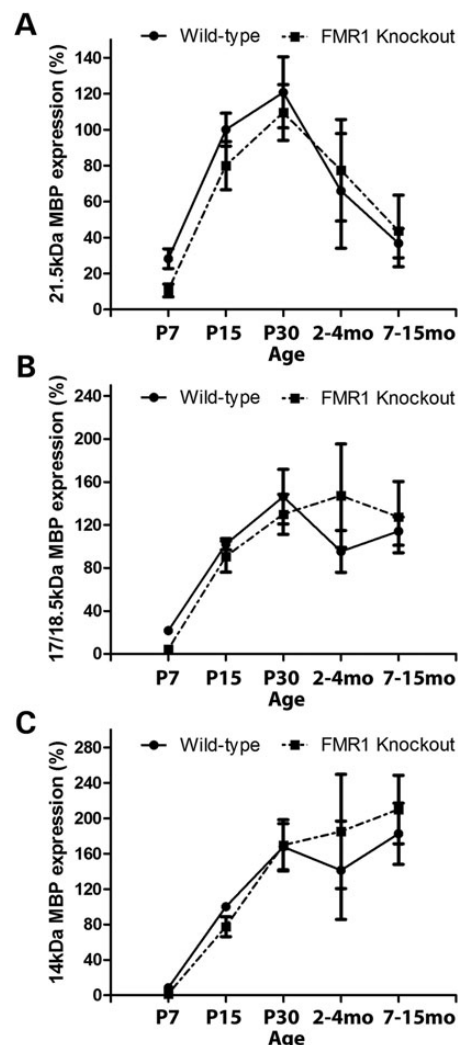
Figure 3. MBP expression in the Fmr1 cerebellum. Quantitative western blotting of wild-type and Fmr1 cerebellum revealed a significant decrease in the expression of MBP in Fmr1 mice at PND 7 (**A**) and PND 15 (**B**). Immunofluorescence staining also demonstrated reduced MBP expression in the deep cerebellar white matter at PND 7 (A). No significant differences in expression were evident at PND 30 (**C**), but MBP expression .... Fmr1 cerebellum (**D**). In (A), DCN, deep cerebellar nuclei; WM, white matter; scale bar = 100 μm. $n = 4–16$ per genotype. *$P < 0.05$; **$P < 0.01$.

Figure 4. MBP expression over development. Quantitative western blotting was used to quantify the expression of the 21.5 kDa (**A**), 17.5/18.5 kDa (**B**) and 14 kDa (**C**) isoforms of MBP over development in wild-type (circle) and Fmr1 (squares with dotted line) cerebellum. Expression of MBP isoforms was quantified relative to expression in PND15 wild-type cerebellum. Fmr1 mice show a rightward shift in MBP expression over development, suggesting a delay in myelination in these mice relative to wild-type animals. $n = 4$ per age per genotype.

proliferation and differentiation *in vitro* (37). This suggests that, in addition to correcting FXS-related phenotypes such as audiogenic seizures and abnormal dendritic spine morphology (38,39), early treatment with R-baclofen might also be beneficial in treating the delayed myelination observed in Fmr1 mice.

## RNA-binding proteins regulate the expression of myelin proteins

Post-transcriptional regulation of myelin protein expression has been shown to be a key regulatory mechanism in ensuring proper myelin formation (40). The RNA-binding protein QKI regulates the expression of several myelin associated proteins, including MBP (41,42). *Quaking* mice, which have a mutation that reduces QKI expression in oligodendrocytes, have a deficit in compact myelin that results in tremors in their hindquarters during movement (43). These mice also have significantly reduced expression of MBP which results from destabilization and mis-localization of MBP mRNA in the cytoplasm of oligodendrocytes (41).

Given the role of FMRP in regulating protein expression, it is not surprising it is important for proper myelination. We have demonstrated that OPCs and some oligodendrocytes express FMRP in the PND 7 cerebellum. Wang *et al.* (16) reported that OPCs, but not mature oligodendrocytes, express FMRP and the decline in FMRP levels during maturation was correlated with an increase in MBP expression. This group also demonstrated that FMRP binds to and regulates the translation of MBP mRNA *in vitro*. Using different experimental strategies, several other groups have also identified the mRNAs for MBP and CNPase (another myelin protein) as substrates for FMRP (1,44). We observed a dramatic decrease in the protein expression of MBP and CNPase in young Fmr1 cerebellum, suggesting
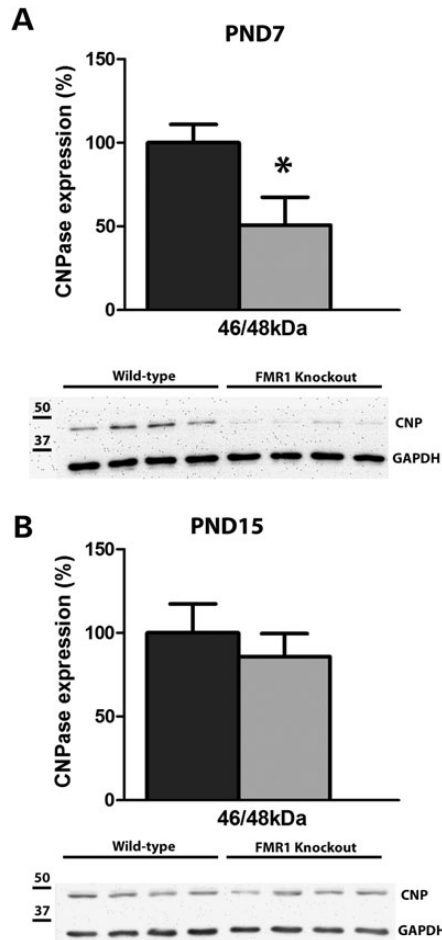
Figure 5. CNPase expression in the Fmr1 cerebellum. Quantitative western blotting of WT and Fmr1 cerebellum revealed a significant decrease in the expression of 2′,3′-cyclic-nucleotide 3′-phosphodiesterase (CNPase), a major component of myelin, in Fmr1 mice at PND 7 (**A**). No significant differences in CNPase expression were detected at PND15 (**B**). $n = 4-8$ per genotype. *$P < 0.05$.

that, in the absence of FMRP, inappropriate regulation of the expression of these (and potentially other, as yet unidentified proteins) may result in the delayed myelination that we observed in Fmr1 mice.

In addition to being an important component of myelin, CNPase is also an RNA-binding protein that can regulate mRNA translation (45), although its mRNA targets have not yet been established. Therefore, in addition to indicating a reduction in mature myelin, under-expression of CNPase could also have functional consequences in Fmr1 cerebellum owing to its role in regulating protein translation.

Neuronal activity regulates myelination

Neuronal activity is an important regulator of myelination and it is conceivable that altered neuronal activity could influence myelination in FXS. OPCs can undergo depolarization in response to neuronal activation (46). While the role of depolarization in OPCs is currently unclear, both proliferation and differentiation of OPCs can be inhibited *in vitro* by treatment with glutamate (47). This finding suggests that glutamate

signaling may limit myelination through its action on OPCs. Neuronal hyperexcitability is well established in FXS (15,29,38,48,49), although it is unclear how early in development this hyperexcitability is established. It is possible that early neuronal hyperexcitability could affect myelination, thereby contributing to the abnormal neuronal structure and/or function commonly seen later in development. However, the profound deficit that we report here in myelin production in the Fmr1 mouse cerebellum in the first 1−2 postnatal weeks is in contrast to the relatively more subtle effects reported in neurons at these early timepoints. For example, recent studies have revealed somewhat mild changes in dendritic spines (50) and cortical maturation (51) at PND 7 in Fmr1 mice. Therefore, altered myelination might precede and possibly contribute to, neuronal abnormalities. Further studies of neurons and oligodendrocytes are needed to determine the interplay between these two cells types in FXS.

The importance of proper myelination during development

The timing of axonal myelination is critical for the normal development of neurons (52). Of note is the observation of delayed myelination in a maternal immune activation model of autism where the offspring from female mice challenged with lipopolysaccharide during pregnancy showed a delay in myelination in the immature brain that was normalized several weeks later, a situation similar to what we report here in Fmr1 mice (53). This group, and others who have used this model, report abnormal behaviors that are thought to reflect autistic-like behaviors in rodents, including altered motor activity, pre-pulse inhibition and anxiety (54,55), suggesting a possible link between abnormal myelin and many of the phenotypes common to autism and FXS.

Few studies to date have addressed the importance of early myelin/white matter deposition for the proper growth and development of the human brain. Steele *et al.* (56) demonstrated the importance of early white matter development in musicians. Using diffusion tensor imaging to compare white matter organization between musicians who began training before age 7, and those who began after age 7, the authors identified a 'sensitive period where experience produces long-lasting changes in the brain and behaviour' such that early musical training has differential impact on (increasing) white matter deposition and 'sensorimotor synchronization performance.' This study and others (e.g. 57,58) demonstrate a critical window for myelin deposition that affects the structure and function of the brain well into adulthood. By extension, it is possible that if myelin deposition is reduced during this critical early postnatal period (as documented here in the Fmr1 mouse brain), it could leave lasting structural and behavioral deficits even as myelin levels normalize.

CONCLUSIONS

Our results reveal a delay in myelination accompanied by reduced OPC number and smaller cerebellar volume in Fmr1 mice during early postnatal development. The results reported here, together with emerging evidence from imaging studies conducted on humans with FXS and idiopathic autism, indicate
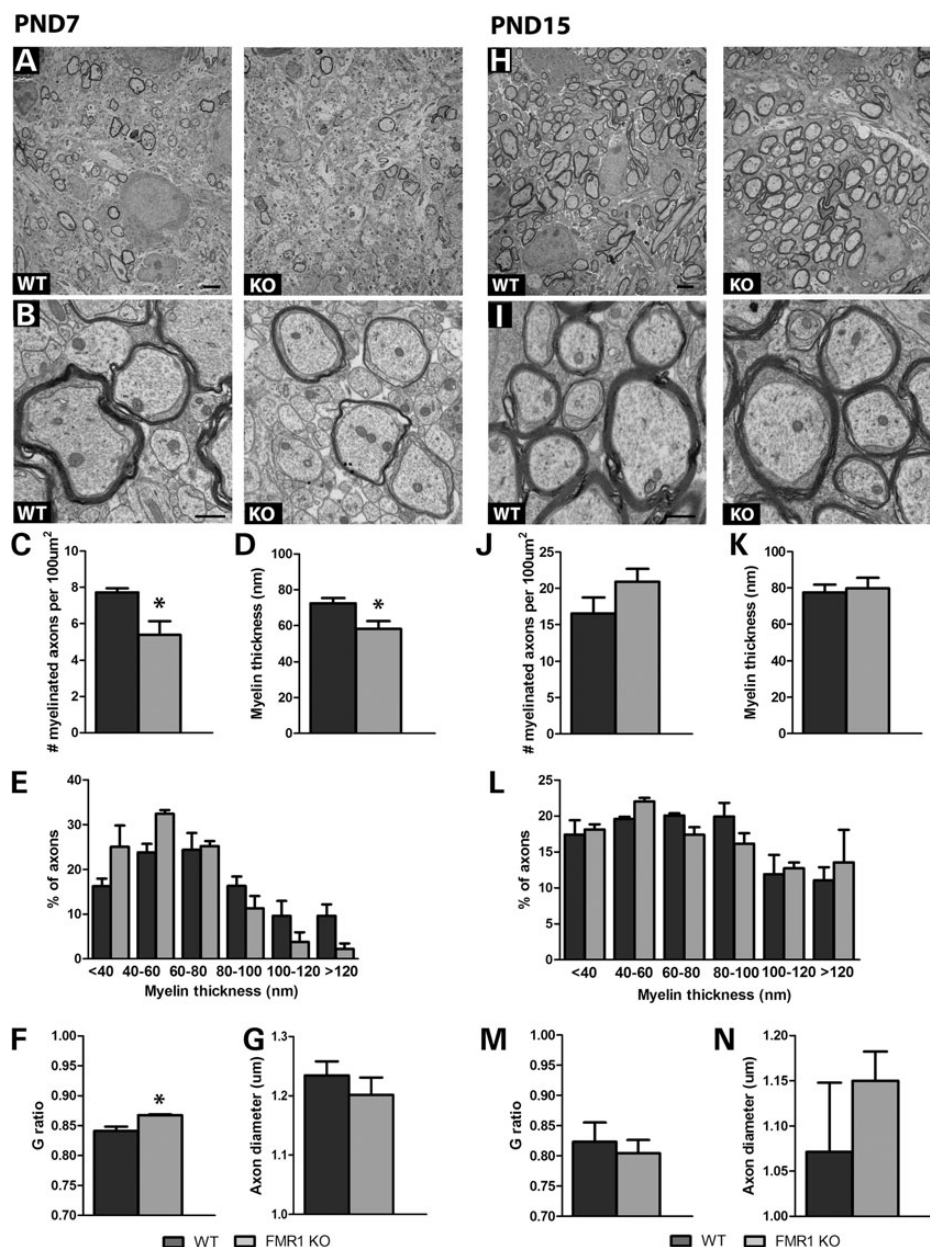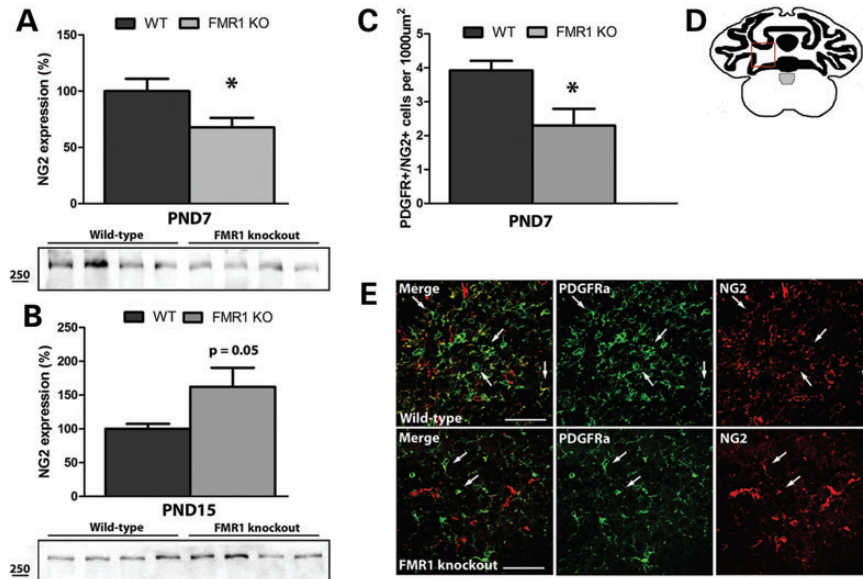
Figure 6. Electron microscopy of PND 7 and PND 15 cerebellar axons. (**A** and **H**) Photomicrographs of wild-type and Fmr1 knockout cerebellum showing fewer myelinated axons in Fmr1 cerebellum at PND 7 (A) but not PND15 (H) compared with wild-type. (**B** and **I**) Higher magnification images of wild-type and Fmr1 knockout showing a reduction in myelin thickness in Fmr1 axons at PND 7 (B) but no difference at PND15 (I). (**C**–**G**) Histograms showing significantly fewer myelinated axons (C), reduced myelin thickness (D), an altered distribution of myelin thicknesses (E), increased G-ratio (F) and no difference in axon diameter (G) in Fmr1 knockout mice compared with wild-type at PND 7. No significant differences in these parameters were seen at PND 15 (**J**–**N**). $n = 2-3$ per genotype. Scale bars in (A) and (F) = 2 μm; scale bars in (B) and (G) = 500 nm. $^*P < 0.05$; $^{**}P < 0.01$.

MATERIALS AND METHODS

Animals

All animal experiments were carried out in accordance with the guidelines set out by the Canadian Council on Animal Care and were approved by the University of Toronto Animal Care Committee. Wild-type C57BL/6 and Fmr1 knockout mice (backcrossed >10 generations on the C57BL/6 background) were generously provided by Dr William Greenough, University of Illinois, and bred at the University of Toronto. All mice were the off-spring

that white matter abnormalities may represent a common early disturbance in neurodevelopmental disorders. Although deterioration of myelin is a hallmark of multiple sclerosis and other de-myelinating disorders affecting adolescents and adults, the consequences of delayed myelination during brain development are less well understood (52,58). Further investigations into the role of FMRP in OPCs, and the dynamic relationship between delayed myelination and FXS-related neuronal abnormalities have the potential to lead to a better understanding of the under-lying neuropathology of FXS.

Figure 7. OPCs in the young mouse cerebellum. Western blots of whole cerebellum using an antibody to the oligodendrocyte precursor cell (OPC) marker NG2 demonstrated a reduction in NG2 expression in the cerebellum of Fmr1 knockout mice at PND 7 compared with wild-type (**A**). In contrast, at PND 15, NG2 expression was elevated in the Fmr1 cerebellum (**B**). NG2 expression was below the level of detection in the samples of cerebellum from PND 30 and adult wild-type and Fmr1 mice. (**C**) Immunocytochemical analysis revealed that the number of OPCs double labeled for NG2 and PDGFRα was significantly reduced in Fmr1 knockout mice at PND 7 compared with wild-type. (**D**) Schematic diagram showing the location of the deep white matter from which OPC numbers were quantified. (**E**) Representative images of NG2/PDGFRα staining in PND 7 cerebellum. $n = 8$ per genotype for western blot; $n = 3$ per genotype for immunocytochemistry. *$P < 0.05$.

of homozygous pairings. Animals were gender-matched within each experiment and the data presented represents a combination of results from matched male and female mice.

Immunocytochemistry

PND 15, 30 or adult (2–4 months) wild-type and Fmr1 knockout mice were anaesthetized with ketamine/xylazine and intracardially perfused with 0.1M PBS followed by 4% paraformaldehyde. Brains were removed and post-fixed overnight in 4% PFA at 4°C. Brains were subsequently rinsed with PBS and sunk in 30% sucrose/PBS overnight at 4°C. The cerebellum was removed, embedded in OCT and sectioned with a cryostat. Floating coronal cerebellar sections (25 μm) were rinsed in PBS then blocked for 1 h at room temperature in PBS containing 5% goat serum and 0.2% triton X-100. After three 5 min washes, sections were incubated in primary antibody overnight at 4°C. Sections were washed 5 × 10 min in PBS then incubated in secondary antibody for 2 h at room temperature. After 5 × 10 min washes, sections were mounted on glass slides with Prolong Gold Antifade (Invitrogen). For NG2/PDGFRα double labeling, perfused PND 7 brains were placed directly in 30% sucrose (no post-fix) overnight and 14 μm frozen sections were mounted on Superfrost® (VWR) slides and treated as described earlier.

For sections treated with the 2F5 anti-FMRP antibody, antigen retrieval was performed as described by Gabel *et al*. (59). Briefly, floating sections were treated with 0.8% sodium borohydride, washed with PBS then incubated for 45 min at 75°C in 0.01 M Na citrate, pH 6.0. After cooling to room temperature, sections were rinsed with PBS, blocked and treated with primary and secondary antibodies as described earlier.

All primary and secondary antibodies were diluted in 0.1 M PBS containing 5% goat serum. Primary antibodies included

rat-anti MBP (1:1000, Millipore); rat -anti PDGFRα (1:100, BD Pharmigen); rabbit anti-NG2 (1:250; Millipore); mouse monoclonal anti-FMRP (clone 2F5-1, 1:1000, gift of Dr J. Darnell). Secondary antibodies were goat anti-mouse Alexa-Fluor 488 (1:2000); goat anti-rabbit AlexaFluor 594 (1:1000); anti-rat AlexaFluor 488 (1:500).

For co-localization of PDGFRα and NG2, digital images of the deep white matter of the cerebellum (Fig. 7D) were captured using a Nikon A1R Confocal Laser Microscope System driven by the Nikon Elements software package. The analysed sections corresponded approximately to the region between the coordinates −8.79 mm bregma and −9.03 mm bregma according to Paxinos *et al*. (60). Images were processed using Image J software (NIH) and the number of cells in the deep cerebellar white matter expressing both NG2 and PDGFRα was counted and expressed as the number of cells per 1000 μm². A total of three wild-type and three Fmr1 knockout brains were analyzed in pairs and 4–8 separate matched images were analyzed from each pair. An unpaired Student's *t*-test was used to determine statistical significance.

For FMRP co-localization with MBP, NG2 and PDGFRα, 14 μm thaw-mounted cryostat sections from PND 7 wild-type mice were treated as outlined earlier. Digital images of the deep white matter (Fig. 7D) from 4–8 sections per mouse were captured as above and the number of cell bodies co-labeled with FMRP and MBP or NG2 or PDGFR were counted and expressed as a percent of all cell bodies expressing the MBP or NG2 or PDGFRα. $n = 4$ for MBP and NG2 and $n = 3$ for PDGFRα.

Electron microscopy

PND 7 and 15 wild-type and Fmr1 mice were anesthetized with ketamine/xylazine and intra-cardially perfused with 0.1 M PBS

followed by 4% paraformaldehyde plus 1% glutaradehyde (in 0.1 M PBS, pH7.2). The cerebellum was dissected and post-fixed in paraformaldehyde plus glutaraldehyde at room temperature for 2 h after which the fixative was removed and replaced with fresh fixative and the samples were stored at 4°C. After washing, the samples were post-fixed with 1% osmium tetraoxide in PBS for 2 h at room temperature in the dark. The samples were washed with PBS followed by dehydration using a graded series of ethanol/distilled water: 50, 70, 90 and 100% in 45 min, 45 min, 1 h and 2 h, respectively at room temperature. The samples were then washed with propylene oxide and infiltrated with Spurrs resin using a graded series of Spurrs and Propylene oxide mixture: (i) one part Spurrs resin mixed with two parts 100% PO for 2 h using an agitator; (ii) two parts Spurrs resin mixed with one part 100% PO for 3 h using an agitator; (iii) 100% Spurrs overnight using an agitator; (iv) second change with 100% Spurrs resin after the overnight for 2 h. Samples were placed in the mold and polymerized at 60°C for 48 h. After complete polymerization, the sample was sectioned on a Reichert Ultracut E microtome to 90 nm thickness and collected on 200 mesh copper grids. The sections were stained using saturated uranyl acetate for 15 min, rinsed in distilled water, followed by Reynold's lead citrate. The sections were examined and the deep cerebellar white matter was photographed in a Hitachi H7000 transmission electron microscope at an accelerating voltage of 75 kV. Images were analyzed using Image J software. For each animal, the number of myelinated neurons were counted in each of 12–14 low magnification images and the average density was calculated (total area per image was 697 μm^2). Using Image J software, myelin thickness was measured for >200 axons from 10 images per mouse. The data were pooled to produce a mean myelin thickness for each animal, or binned to provide an analysis of distribution of myelin thickness.

Whole fiber (axon plus myelin) and axonal areas were measured for >140 axons from six images and used to derive axonal and whole fiber diameters as described previously (61). Longitudinally sectioned fibers were excluded from this analysis. The G ratio, a measure of myelin thickness, was calculated as axonal diameter/whole fiber diameter.

Diffusion tensor imaging

PND 7 wild-type and Fmr1 mice ($n = 10$ per genotype) were intra-cardially perfused with PBS containing 1 μl/ml heparin with 2 mM gadolinium DTPA (ProHance), followed by 4% paraformaldehyde containing 2 mM gadolinium. Skulls were isolated and fixed overnight in 4% paraformaldehyde with 2 mM gadolinium at 4°C. The brains were then kept in PBS with 2 mM gadolinium and 0.02% sodium azide until imaged. Imaging was conducted with Diffusion Tensor Imaging having a resolution of 78 μm and 30 different directions. The high-b images ($b = 1917$ s/mm^2) of all 20 brains were registered by first aligning them in 3-D space to create a consensus average brain. Here the high-b images were used because they offered an increased contrast between the white and grey matter that was not visible in the low-B images. Next, deformation fields that transform each individual brain image to this consensus average image were computed. These deformation fields were utilized in calculating voxel-wise volumetric brain changes.

Volumetric changes of the cerebellum were extracted by tracing in 3D space and computing the 3D volume. After acquisition, the images were analyzed using FSL software package (FMRIB, Oxford, UK), which was used to create Fractional Anisotropy maps for each of the 20 brains imaged.

Western blotting

Quantitative western blotting was performed as previously described (62). The cerebellum was isolated and homogenized in ice cold 50 mM Tris–HCl, 1% SDS, pH 7.4, supplemented with protease inhibitor cocktail (Roche) using a glass/teflon homogenizer. Protein concentrations were determined using the BCA assay (Sigma). Equal amounts of protein (6–30 μg depending on the abundance of the target protein) were loaded onto a 6, 10 or 12% polyacrylamide–SDS gel and transferred onto a nitrocellulose membrane after electrophoresis. The membranes were blocked in 5% milk for 1 h and incubated at 4°C overnight with one of the following primary antibodies: rat anti-MBP (1:1000; Millipore), rabbit anti-NG2 (1:250; Millipore) or mouse anti-CNPase (1: 500, Millipore) and mouse anti-GAPDH antibody (1:40 000–1:100 000; Sigma). After washing, a goat anti-mouse, goat anti-rabbit or goat anti-rat (Jackson Labs) HRP-conjugated secondary antibody was applied for 2 h. The immunoreactive proteins were visualized using the FluorChem^TM MultiImage Light Cabinet (Alpha Innotech). Densitometric analysis was carried out using the AlphaEaseFC software (Alpha Innotech). The intensity of the band of interest was normalized relative to the GAPDH band intensity. Protein expression in WT and Fmr1 knockout animals is presented as a percentage of wild-type expression levels. An unpaired Student's t-test was performed to determine statistical significance.

REFERENCES

1. Darnell, J.C., Van Driesche, S.J., Zhang, C., Hung, K.Y., Mele, A., Fraser, C.E., Stone, E.F., Chen, C., Fak, J.J., Chi, S.W. *et al.* (2011) FMRP stalls ribosomal translocation on mRNAs linked to synaptic function and autism. *Cell*, **146**, 247–261.
2. Bassell, G.J. and Warren, S.T. (2008) Fragile X syndrome: loss of local mRNA regulation alters synaptic development and function. *Neuron*, **60**, 201–214.
3. Rooms, L. and Kooy, R.F. (2011) Advances in understanding fragile X syndrome and related disorders. *Curr. Opin. Pediatr.*, **23**, 601–606.
4. Hampson, D.R., Gholizadeh, S. and Pacey, L.K. (2012) Pathways to drug development for autism spectrum disorders. *Clin. Pharmacol. Ther.*, **91**, 189–200.
5. Mostofsky, S.H., Mazzocco, M.M., Aakalu, G., Warsofsky, I.S., Denckla, M.B. and Reiss, A.L. (1998) Decreased cerebellar posterior vermis size in

fragile X syndrome: correlation with neurocognitive performance. *Neurology*, **50**, 121–130.

6. Hoeft, F., Carter, J.C., Lightbody, A.A., Cody, H.H., Piven, J. and Reiss, A.L. (2010) Region-specific alterations in brain development in one- to three-year-old boys with fragile X syndrome. *Proc. Natl Acad. Sci. USA*, **107**, 9335–9339.

7. Greco, C.M., Navarro, C.S., Hunsaker, M.R., Maezawa, I., Shuler, J.F., Tassone, F., Delany, M., Au, J.W., Berman, R.F., Jin, L.W. *et al.* (2011) Neuropathologic features in the hippocampus and cerebellum of three older men with fragile X syndrome. *Mol. Autism*, **2**, 2.

8. Kaufmann, W.E., Cooper, K.L., Mostofsky, S.H., Capone, G.T., Kates, W.R., Newschaffer, C.J., Bukelis, I., Stump, M.H., Jann, A.E. and Lanham, D.C. (2003) Specificity of cerebellar vermian abnormalities in autism: a quantitative magnetic resonance imaging study. *J. Child Neurol.*, **18**, 463–470.

9. Whitney, E.R., Kemper, T.L., Bauman, M.L., Rosene, D.L. and Blatt, G.J. (2008) Cerebellar Purkinje cells are reduced in a subpopulation of autistic brains: a stereological experiment using calbindin-D28k. *Cerebellum*, **7**, 406–416.

10. Schumann, C.M. and Nordahl, C.W. (2011) Bridging the gap between MRI and postmortem research in autism. *Brain Res.*, **1380**, 175–186.

11. Ellegood, J., Pacey, L.K., Hampson, D.R., Lerch, J.P. and Henkelman, R.M. (2010) Anatomical phenotyping in a mouse model of fragile X syndrome with magnetic resonance imaging. *Neuroimage*, **53**, 1023–1029.

12. Tsai, P.T., Hull, C., Chu, Y., Greene-Colozzi, E., Sadowski, A.R., Leech, J.M., Steinberg, J., Crawley, J.N., Regehr, W.G. and Sahin, M. (2012) Autistic-like behaviour and cerebellar dysfunction in Purkinje cell Tsc1 mutant mice. *Nature*, **488**, 647–651.

13. Reith, R.M., McKenna, J., Wu, H., Hashmi, S.S., Cho, S.H., Dash, P.K. and Gambello, M.J. (2013) Loss of Tsc2 in Purkinje cells is associated with autistic-like behavior in a mouse model of tuberous sclerosis complex. *Neurobiol. Dis.*, **51**, 93–103.

14. Pacey, L.K. and Doering, L.C. (2007) Developmental expression of FMRP in the astrocyte lineage: implications for fragile X syndrome. *Glia*, **55**, 1601–1609.

15. Higashimori, H., Morel, L., Huth, J., Lindemann, L., Dulla, C., Taylor, A., Freeman, M. and Yang, Y. (2013) Astroglial FMRP-dependent translational down-regulation of mGluR5 underlies glutamate transporter GLT1 dysregulation in the fragile X mouse. *Hum. Mol. Genet.*, **22**, 2041–2054.

16. Wang, H., Ku, L., Osterhout, D.J., Li, W., Ahmadian, A., Liang, Z. and Feng, Y. (2004) Developmentally-programmed FMRP expression in oligodendrocytes: a potential role of FMRP in regulating translation in oligodendroglia progenitors. *Hum. Mol. Genet.*, **13**, 79–89.

17. Callan, M.A., Clements, N., Ahrendt, N. and Zarnescu, D.C. (2012) Fragile X Protein is required for inhibition of insulin signaling and regulates glial-dependent neuroblast reactivation in the developing brain. *Brain Res.*, **1462**, 151–161.

18. Barnea-Goraly, N., Eliez, S., Hedeus, M., Menon, V., White, C.D., Moseley, M. and Reiss, A.L. (2003) White matter tract alterations in fragile X syndrome: preliminary evidence from diffusion tensor imaging. *Am. J. Med. Genet. B Neuropsychiatr. Genet.*, **118B**, 81–88.

19. Haas, B.W., Barnea-Goraly, N., Lightbody, A.A., Patnaik, S.S., Hoeft, F., Hazlett, H., Piven, J. and Reiss, A.L. (2009) Early white-matter abnormalities of the ventral frontostriatal pathway in fragile X syndrome. *Dev. Med. Child Neurol.*, **51**, 593–599.

20. Groen, W.B., Buitelaar, J.K., van der Gaag, R.J. and Zwiers, M.P. (2011) Pervasive microstructural abnormalities in autism: a DTI study. *J. Psychiatry Neurosci.*, **36**, 32–40.

21. Singh, K., Gaur, P. and Prasad, S. (2007) Fragile x mental retardation (Fmr-1) gene expression is down regulated in brain of mice during aging. *Mol. Biol. Rep.*, **34**, 173–181.

22. Alger, J.R. (2012) The diffusion tensor imaging toolbox. *J. Neurosci.*, **32**, 7418–7428.

23. Fitzner, D., Schneider, A., Kippert, A., Mobius, W., Willig, K.I., Hell, S.W., Bunt, G., Gaus, K. and Simons, M. (2006) Myelin basic protein-dependent plasma membrane reorganization in the formation of myelin. *EMBO J.*, **25**, 5037–5048.

24. Brady, S.T., Witt, A.S., Kirkpatrick, L.L., de Waegh, S.M., Readhead, C., Tu, P.H. and Lee, V.M. (1999) Formation of compact myelin is required for maturation of the axonal cytoskeleton. *J. Neurosci.*, **19**, 7278–7288.

25. Polito, A. and Reynolds, R. (2005) NG2-expressing cells as oligodendrocyte progenitors in the normal and demyelinated adult central nervous system. *J. Anat.*, **207**, 707–716.

26. Kucharova, K. and Stallcup, W.B. (2010) The NG2 proteoglycan promotes oligodendrocyte progenitor proliferation and developmental myelination. *Neuroscience*, **166**, 185–194.

27. Stallcup, W.B. (2002) The NG2 proteoglycan: past insights and future prospects. *J. Neurocytol.*, **31**, 423–435.

28. Foran, D.R. and Peterson, A.C. (1992) Myelin acquisition in the central nervous system of the mouse revealed by an MBP-Lac Z transgene. *J. Neurosci.*, **12**, 4890–4897.

29. Hagerman, R., Hoem, G. and Hagerman, P. (2010) Fragile X and autism: intertwined at the molecular level leading to targeted treatments. *Mol. Autism*, **1**, 12.

30. Rosenberg, S.S., Kelland, E.E., Tokar, E., De la Torre, A.R. and Chan, J.R. (2008) The geometric and spatial constraints of the microenvironment induce oligodendrocyte differentiation. *Proc. Natl Acad. Sci. USA*, **105**, 14662–14667.

31. Simons, M. and Trajkovic, K. (2006) Neuron-glia communication in the control of oligodendrocyte function and myelin biogenesis. *J. Cell Sci.*, **119**, 4381–4389.

32. Trapp, B.D. and Kidd, G.J. (2000) Axo-glial septate junctions. The maestro of nodal formation and myelination? *J. Cell Biol.*, **150**, F97–F100.

33. Voyvodic, J.T. (1989) Target size regulates calibre and myelination of sympathetic axons. *Nature*, **342**, 430–433.

34. Berry-Kravis, E.M., Hessl, D., Rathmell, B., Zarevics, P., Cherubini, M., Walton-Bowen, K., Mu, Y., Nguyen, D.V., Gonzalez-Heydrich, J., Wang, P.P. *et al.* (2012) Effects of STX209 (arbaclofen) on neurobehavioral function in children and adults with fragile X syndrome: a randomized, controlled, phase 2 trial. *Sci. Transl. Med.*, **4**, 152ra127.

35. Michalon, A., Sidorov, M., Ballard, T.M., Ozmen, L., Spooren, W., Wettstein, J.G., Jaeschke, G., Bear, M.F. and Lindemann, L. (2012) Chronic pharmacological mGlu5 inhibition corrects fragile X in adult mice. *Neuron*, **74**, 49–56.

36. Luyt, K., Varadi, A., Durant, C.F. and Molnar, E. (2006) Oligodendroglial metabotropic glutamate receptors are developmentally regulated and involved in the prevention of apoptosis. *J. Neurochem.*, **99**, 641–656.

37. Luyt, K., Slade, T.P., Dorward, J.J., Durant, C.F., Wu, Y., Shigemoto, R., Mundell, S.J., Varadi, A. and Molnar, E. (2007) Developing oligodendrocytes express functional GABA(B) receptors that stimulate cell proliferation and migration. *J. Neurochem.*, **100**, 822–840.

38. Pacey, L.K., Heximer, S.P. and Hampson, D.R. (2009) Increased GABA(B) receptor-mediated signaling reduces the susceptibility of fragile X knockout mice to audiogenic seizures. *Mol. Pharmacol.*, **76**, 18–24.

39. Henderson, C., Wijetunge, L., Kinoshita, M.N., Shumway, M., Hammond, R.S., Postma, F.R., Brynczka, C., Rush, R., Thomas, A., Paylor, R. *et al.* (2012) Reversal of disease-related pathologies in the fragile X mouse model by selective activation of GABA(B) receptors with arbaclofen. *Sci. Transl. Med.*, **4**, 152ra128.

40. Harauz, G. and Boggs, J.M. (2013) Myelin management by the 18.5-kDa and 21.5-kDa classic myelin basic protein isoforms. *J. Neurochem.*, **125**, 334–361.

41. Li, Z., Zhang, Y., Li, D. and Feng, Y. (2000) Destabilization and mislocalization of myelin basic protein mRNAs in quaking dysmyelination lacking the QKI RNA-binding proteins. *J. Neurosci.*, **20**, 4944–4953.

42. Zhang, Y. and Feng, Y. (2001) Distinct molecular mechanisms lead to diminished myelin basic protein and 2′,3′-cyclic nucleotide 3′-phosphodiesterase in qk(v) dysmyelination. *J. Neurochem.*, **77**, 165–172.

43. Zearfoss, N.R., Farley, B.M. and Ryder, S.P. (2008) Post-transcriptional regulation of myelin formation. *Biochim. Biophys. Acta*, **1779**, 486–494.

44. Ascano, M., Mukherjee, N., Bandaru, P., Miller, J.B., Nusbaum, J.D., Corcoran, D.L., Langlois, C., Munschauer, M., Dewell, S., Hafner, M. *et al.* (2012) FMRP targets distinct mRNA sequence elements to regulate protein expression. *Nature*, **492**, 382–386.

45. Gravel, M., Robert, F., Kottis, V., Gallouzi, I.E., Pelletier, J. and Braun, P.E. (2009) 2′,3′-Cyclic nucleotide 3′-phosphodiesterase: a novel RNA-binding protein that inhibits protein synthesis. *J. Neurosci. Res.*, **87**, 1069–1079.

46. Emery, B. (2010) Regulation of oligodendrocyte differentiation and myelination. *Science*, **330**, 779–782.

47. Gallo, V., Zhou, J.M., McBain, C.J., Wright, P., Knutson, P.L. and Armstrong, R.C. (1996) Oligodendrocyte progenitor cell proliferation and lineage progression are regulated by glutamate receptor-mediated K+ channel block. *J. Neurosci.*, **16**, 2659–2670.

48. Gross, C., Yao, X., Pong, D.L., Jeromin, A. and Bassell, G.J. (2011) Fragile x mental retardation protein regulates protein expression and mRNA translation of the potassium channel kv4.2. *J. Neurosci.*, **31**, 5693–5698.

49. Olmos-Serrano, J.L., Paluszkiewicz, S.M., Martin, B.S., Kaufmann, W.E., Corbin, J.G. and Huntsman, M.M. (2010) Defective GABAergic neurotransmission and pharmacological rescue of neuronal hyperexcitability in the amygdala in a mouse model of fragile X syndrome. *J. Neurosci.*, **30**, 9929–9938.

50. Cruz-Martin, A., Crespo, M. and Portera-Cailliau, C. (2012) Glutamate induces the elongation of early dendritic protrusions via mGluRs in wild type mice, but not in fragile X mice. *PLoS. One.*, **7**, e32446.

51. Till, S.M., Wijetunge, L.S., Seidel, V.G., Harlow, E., Wright, A.K., Bagni, C., Contractor, A., Gillingwater, T.H. and Kind, P.C. (2012) Altered maturation of the primary somatosensory cortex in a mouse model of fragile X syndrome. *Hum. Mol. Genet.*, **21**, 2143–2156.

52. Fields, R.D. (2008) White matter matters. *Sci. Am.*, **298**, 42–49.

53. Makinodan, M., Tatsumi, K., Manabe, T., Yamauchi, T., Makinodan, E., Matsuyoshi, H., Shimoda, S., Noriyama, Y., Kishimoto, T. and Wanaka, A. (2008) Maternal immune activation in mice delays myelination and axonal development in the hippocampus of the offspring. *J. Neurosci. Res.*, **86**, 2190–2200.

54. Malkova, N.V., Yu, C.Z., Hsiao, E.Y., Moore, M.J. and Patterson, P.H. (2012) Maternal immune activation yields offspring displaying mouse versions of the three core symptoms of autism. *Brain Behav. Immun.*, **26**, 607–616.

55. Rana, S.A., Aavani, T. and Pittman, Q.J. (2012) Sex effects on neurodevelopmental outcomes of innate immune activation during prenatal and neonatal life. *Horm. Behav.*, **62**, 228–236.

56. Steele, C.J., Bailey, J.A., Zatorre, R.J. and Penhune, V.B. (2013) Early musical training and white-matter plasticity in the corpus callosum: evidence for a sensitive period. *J. Neurosci.*, **33**, 1282–1290.

57. Makinodan, M., Rosen, K.M., Ito, S. and Corfas, G. (2012) A critical period for social experience-dependent oligodendrocyte maturation and myelination. *Science*, **337**, 1357–1360.

58. Miller, D.J., Duka, T., Stimpson, C.D., Schapiro, S.J., Baze, W.B., McArthur, M.J., Fobbs, A.J., Sousa, A.M., Sestan, N., Wildman, D.E. *et al.* (2012) Prolonged myelination in human neocortical evolution. *Proc. Natl Acad. Sci. USA*, **109**, 16480–16485.

59. Gabel, L.A., Won, S., Kawai, H., McKinney, M., Tartakoff, A.M. and Fallon, J.R. (2004) Visual experience regulates transient expression and dendritic localization of fragile X mental retardation protein. *J. Neurosci.*, **24**, 10579–10583.

60. Paxinos, G., Halliday, G.M., Watson, C., Koucherov, Y. and Wang, H. (2007) *Atlas of the Developing Mouse Brain at E17.5, P0 and P6*. Elsevier, New York, NY.

61. Williams, R.W. and Chalupa, L.M. (1983) An analysis of axon caliber within the optic nerve of the cat: evidence of size groupings and regional organization. *J. Neurosci.*, **3**, 1554–1564.

62. Adusei, D.C., Pacey, L.K., Chen, D. and Hampson, D.R. (2010) Early developmental alterations in GABAergic protein expression in fragile X knockout mice. *Neuropharmacology*, **59**, 167–171.